Use of Ellipsometry in a Study of the Surface Order in the Isotropic Phase of a Liquid Crystalline Polyacrylate

S. Immerschitt, W. Stille,* and G. Strobl

Fakultät für Physik, Universität Freiburg, 7800 Freiburg, Germany

Received October 15, 1991; Revised Manuscript Received February 22, 1992

ABSTRACT: Pretransitional order at the free surface of the isotropic phase of a liquid crystalline side-group polyacrylate was studied by reflection ellipsometry. A large shift of the Brewster angle φ_B to higher values was observed when the temperature approached the isotropic–nematic transition point, indicating a boundary layer of large thickness together with negative anisotropy of the dielectric constant. To describe the profile of the reflecting layer, a model function for the dielectric constant assuming uniaxial symmetry of the layer and exponential decay of the anisotropy was used, taking into account a roughness of the surface. The data are well represented by fits to the model, leading to negative values of the nematic order parameter at the surface.

1. Introduction

The surface of liquid crystals is very sensitive with regard to the boundary condition. Close to the surface the order is often different from that in the bulk. Known examples are boundary layers with smectic order in the nematic phase[1] or layers with smectic[2] or nematic[3–5] order in the isotropic phase. Studies concern in most cases substrate–liquid interfaces. There are also some observations of a special order at free surfaces, i.e., at the liquid–vapor interface. The effects have been discussed in several theoretical treatments.[6–9] As observed, and described by theories, the thickness of the boundary layer increases on approaching the temperature of the phase transitions. In the vicinity of the isotropic–nematic or nematic–smectic phase transitions, which are both weakly first order, two different surface phenomena can occur: "complete wetting" associated with a divergent boundary layer thickness or "near-critical adsorption", leading to a finite thickness at the transition point (for a first-order transition). In the case of near-critical adsorption, the thickness of the boundary layer is given by the correlation length of the order parameter fluctuations in the bulk. Complete wetting introduces an additional length, which is determined by the surface tensions between the coexisting phases.

We recently have performed a study of the state of order at the free surface in the isotropic phase of some low molecular weight and polymeric nematogenic compounds applying ellipsometry. Commercially available ellipsometers work at one or several fixed angles of incidence. Model calculations showed us that the information content of a measurement increases, if the complete angular dependent reflection curves around the Brewster angle are registered. We therefore have built for the study an ellipsometer with a high angular resolution. The investigation concerned the surface properties of two phenylcyclohexanes and of one LC side-group polyacrylate. For the low molecular weight compounds we found clear evidence for a complete wetting of the isotropic phase by a nematic boundary layer with homeotropic order. The results have been presented elsewhere.[10] This report deals with the surface properties of the LC polymer. We found an order different from that of the low molecular compounds, a boundary layer with a planar ordering of the LC groups.

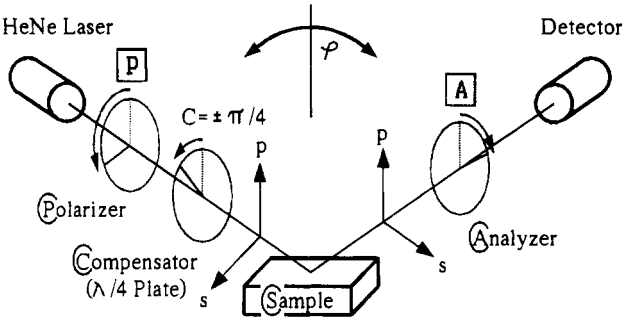

Figure 1. Schematic drawing of a PCSA ellipsometer.

2. Experimental Section

2.1. Ellipsometry. Ellipsometry investigates the state of polarization of a light beam reflected at an interface under variation of the state of polarization of the incident beam. Measurements yield the ratio of the reflection coefficients r_p and r_s for light polarized within and normal to the plan of incidence. The result is expressed using the two ellipsometric quantities tan Ψ and Δ which are defined as

$$r_p/r_s = \tan \Psi e^{i\Delta} \tag{1}$$

We have used a PCSA ellipsometer with a variable angle of incidence. Figure 1 shows a schematic drawing of the apparatus. The quantities Δ and tan Ψ can be derived from the azimuthal angles of the polarizer and analyzer for vanishing transmitted intensity. Details of the techniques are described in the literature.[11] Measurements were performed under variation of the angle of incidence φ in a range of ±1° around the Brewster angle, giving the reflection curves tan $\Psi(\varphi)$ and $\Delta(\varphi)$.

For a steplike change of the dielectric constant ϵ at the interface $\Delta(\varphi)$ and tan $\Psi(\varphi)$ are given by Fresnel's law. If a beam is reflected at the free surface of a liquid with dielectric constant ϵ, r_p and therefore tan Ψ vanish at the Brewster angle φ_B, given by

$$\tan \varphi_B = \epsilon^{1/2} \tag{2}$$

$$\tan \Psi(\varphi_B) = 0 \tag{3}$$

Δ shows a discontinuous change from $\Delta = \pi$ ($\varphi < \varphi_B$) to $\Delta = 0$ ($\varphi > \varphi_B$). Modifications of the profile, as they follow from a special surface structure, lead to deviations from Fresnel's law, which are especially pronounced around φ_B. In general, Δ changes smoothly from π to 0, and tan Ψ does not vanish. In this general case of a structured surface the Brewster angle is defined as

$$\Delta(\varphi_B) = \pi/2 \tag{4}$$

0024-9297/92/2225-3227$03.00/0

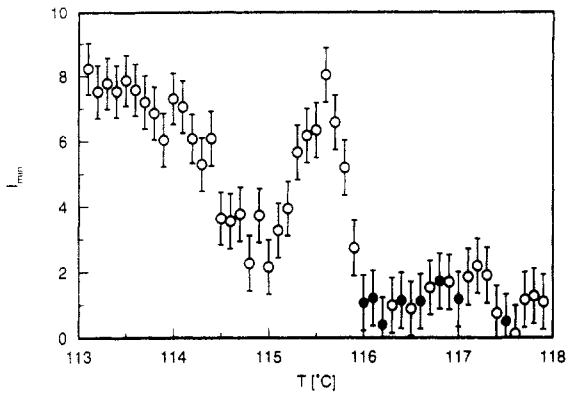

Figure 2. LC-pAc. Unpolarized excess scattering, showing the location of the isotropic–nematic phase transition T_c. Filled symbols indicate the temperatures of ellipsometric measurements.

The minimum of tan Ψ, at an angle φ_{min} with

$$\frac{d \tan \Psi}{d\varphi}(\varphi_{min}) = 0 \tag{5}$$

is called the "ellipticity coefficient". Usually φ_{min} coincides with φ_B or is located very near to it.

2.2. Sample. The sample under investigation was a polyacrylate with a benzoic acid phenylene ester side group (LC-pAc) with the chemical structure

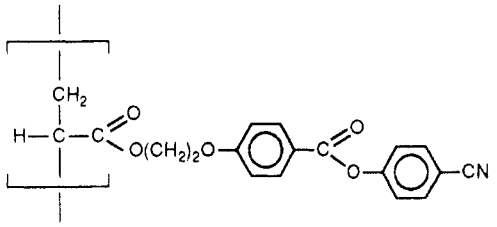

The molecular weight is around 18 000. It was synthesized by R. Zentel (Fachbereich Chemie, Universität Düsseldorf). The compound possesses a nematic phase with a clearing point at T_c = 115.5 °C. The transition from the isotropic to the nematic phase occurs within 0.5 K. The nematic phase is frozen at a glass transition located around 75 °C.

3. Results

In order to determine the transition point, we measured the unpolarized reflected light. Unpolarized excess scattering shows up in the transition region as a result of the two coexisting phases. Figure 2 gives the measured intensity. The clearing point is located at T_c = 115.5 °C. Measurements in the isotropic phase were performed at the eight temperatures indicated by filled symbols. They all lie outside the two-phase region.

Figure 3 shows the reflection curves tan $\Psi(\varphi)$ and $\Delta(\varphi)$, obtained between 116.0 and 117.5 °C. On approaching T_c one observes a slight decrease in the ellipticity coefficient, associated with a comparatively large shift of the Brewster angle to higher values.

The behavior is qualitatively different from that observed on low molecular weight compounds.[5,10] For comparison, Figure 4 gives the curves tan $\Psi(\varphi)$ and $\Delta(\varphi)$ measured for a phenylcyclohexane (PCH5; compare ref 10). Here the change of the ellipticity coefficient on approaching T_c is much larger, but the shift of the Brewster angle is smaller and oriented to smaller angles. Obviously, the state of order in the boundary layer differs between the two samples. For a discussion of the data we have performed calculations of tan $\Psi(\varphi)$ and $\Delta(\varphi)$ for simple model profiles.

4. Model Calculations

Two types of profiles were selected. The first one describes a surface, located at $z = 0$, which is rough rather than atomically flat:

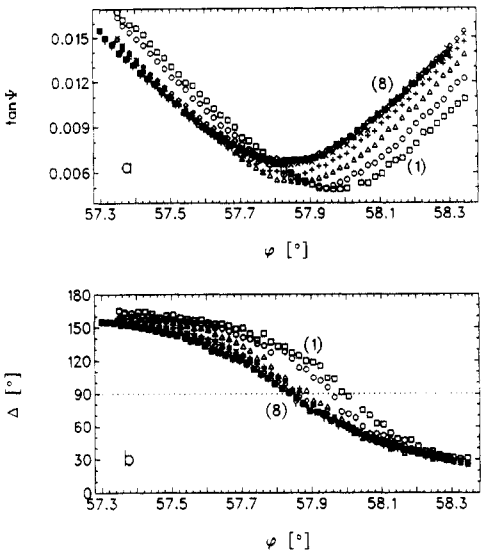

Figure 3. LC-pAc isotropic phase. tan $\Psi(\varphi)$ (a) and $\Delta(\varphi)$ (b) measured in the range of the Brewster angle at different temperatures in the range from T = 116.0 °C (1) to T = 117.5 °C (8) as indicated in Figure 2.

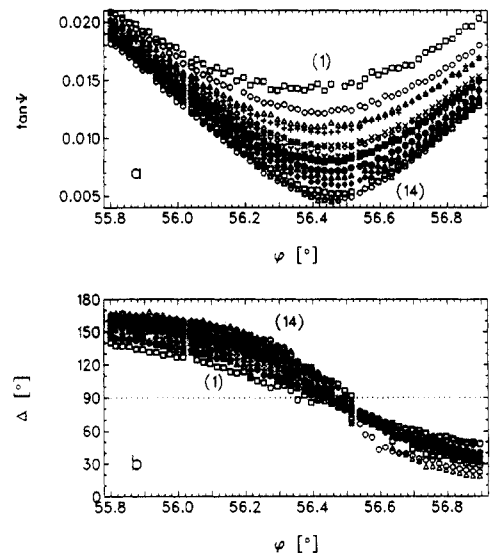

Figure 4. Phenylcyclohexane (PCH5) isotropic phase. tan $\Psi(\varphi)$ (a) and $\Delta(\varphi)$ (b) measured in the range of the Brewster angle at different temperatures near T_c = 55.0 °C (ref 10).

$$\epsilon(z) = 1 + (\epsilon_b - 1)(1 + \tanh(z/\gamma))/2 \tag{6}$$

The parameter γ specifies the roughness; ϵ_b is the bulk dielectric constant. The second profile describes a nematic boundary layer with uniaxial symmetry. Within the layer the dielectric constant is anisotropic, with ϵ_z (polarization along the surface normal) different from ϵ_x (polarization within the surface). We assume an exponential decay of the anisotropy, with a characteristic length ξ:

$$\epsilon_z(z>0) = \epsilon_b + (2/3)\Delta\epsilon \exp(-z/\xi) \tag{7}$$

$$\epsilon_x(z>0) = \epsilon_b - (1/3)\Delta\epsilon \exp(-z/\xi) \tag{8}$$

with

$$\Delta\epsilon = \epsilon_z - \epsilon_x \quad (z = 0) \tag{9}$$

For a given profile the reflectivity curves tan $\Psi(\varphi)$ and $\Delta(\varphi)$ can be determined using the matrix algorithm introduced by Lekner.[12] The surface region is described

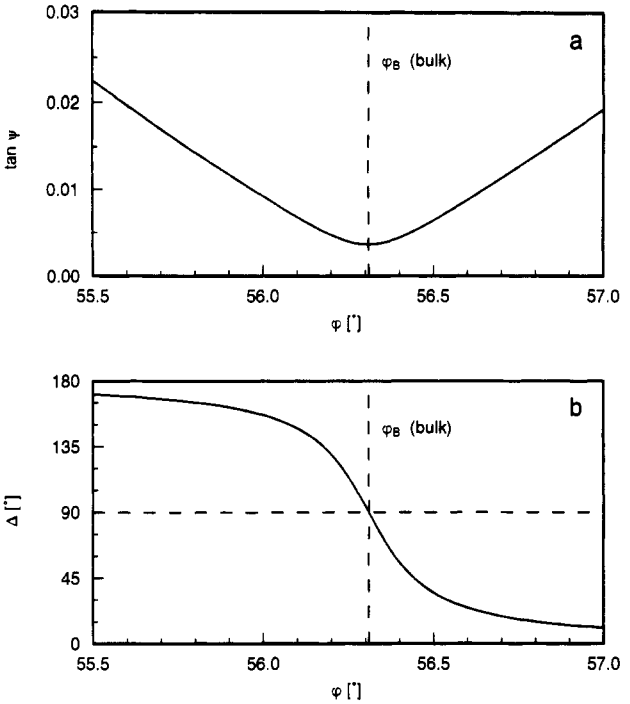

Figure 5. Reflectivity curves tan $\Psi(\varphi)$ (a) and $\Delta(\varphi)$ (b) calculated for the profile in eq 6, choosing $\epsilon_b = 2.25$ and $\gamma = 10$ Å.

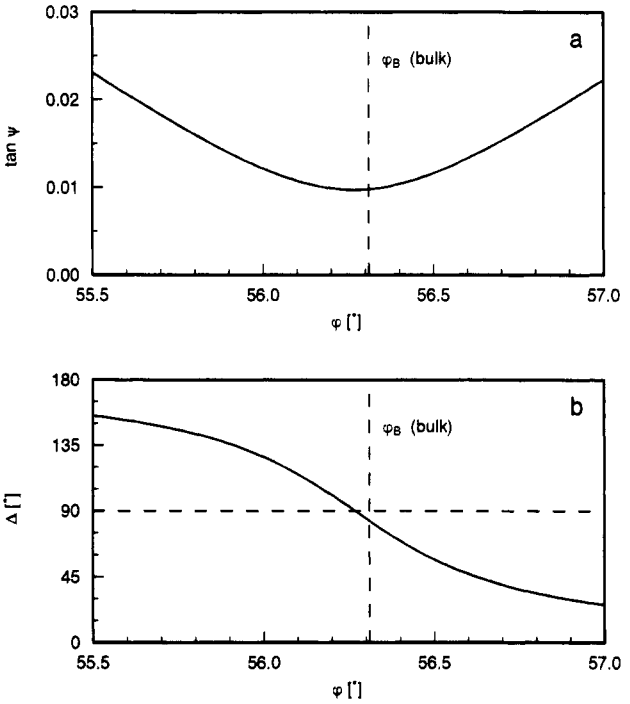

Figure 6. Reflectivity curves tan $\Psi(\varphi)$ (a) and $\Delta(\varphi)$ (b) calculated for the profile in eq 7, choosing $\epsilon_b = 2.25$, $\Delta\epsilon = 0.45$, and $\xi = 50$ Å.

as a set of layers with different internally homogeneous dielectric constants. The total reflectivity follows as a result of the reflections at all interfaces, which can be calculated by a matrix multiplication.

Figures 5–7 show some typical examples, obtained for a wavelength of light of $\lambda = 632.8$ nm. As demonstrated by Figure 5, a surface roughness (here $\gamma = 10$ Å) results in a nonvanishing value of the ellipticity coefficient. It increases with γ. The location of φ_B remains unchanged. The model calculations indicate that, given a simple liquid with a roughened surface, γ can be determined with high precision. This is confirmed by experiments.[13]

Figure 6 demonstrates the effect of a nematic boundary with positive anisotropy, $\Delta\epsilon = 0.45$, and Figure 7 that of

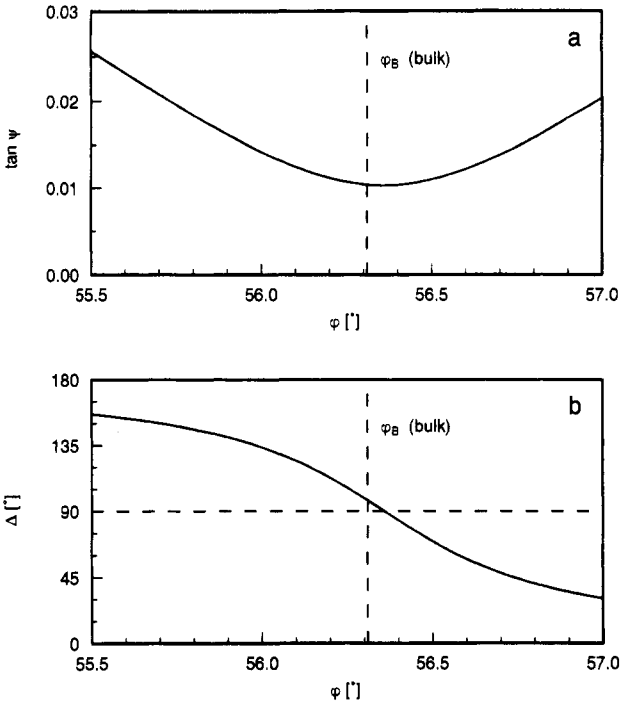

Figure 7. Reflectivity curves tan $\Psi(\varphi)$ (a) and $\Delta(\varphi)$ (b) calculated for the profile in eq 7, choosing $\epsilon_b = 2.25$, $\Delta\epsilon = -0.45$, and $\xi = 50$ Å.

a layer with negative anisotropy, $\Delta\epsilon = -0.45$. In both cases nonvanishing ellipticity coefficients with similar magnitudes are observed. They differ in the direction of the shift of φ_B, going to lower values for $\Delta\epsilon > 0$ and to higher values for $\Delta\epsilon < 0$. Hence, starting a measurement at a temperature away from T_c, where the boundary layer thickness becomes essentially equal to the roughness γ, and observing the shift of φ_B on approaching T_c enable us to discriminate between $\Delta\epsilon > 0$, which usually corresponds to a homeotropic nematic order, and $\Delta\epsilon < 0$, which is indicative of a planar order. Looking at Figure 3, we conclude that the sample under study possesses a boundary layer with planar order, in contrast to the low molecular weight compound (Figure 4), which has a boundary layer with homeotropic order. The decrease of the ellipticity coefficient in Figure 3 is a consequence of the superposition of the roughness of the liquid–vapor interface (eq 6) and the nematic boundary layer (eqs 7 and 8), as will be demonstrated in the following.

It is important to check under which conditions ellipsometric measurements enable a separate determination of the two profile parameters $\Delta\epsilon$ and ξ. Figure 8 shows the result of calculations ($\epsilon_b = 2.25$, $\lambda = 632.8$ nm). The plot gives the dependence of the two measured quantities, the ellipticity coefficient and the Brewster angle, on the model parameters $\Delta\epsilon$ and ξ. Lines for constant values of $\Delta\epsilon$ and ξ are indicated. Also given are typical error bars of a measurement. Use of Figure 8 enables for a given pair of measured quantities, tan $\Psi(\varphi_B)$ and φ_B, determination of $\Delta\epsilon$ and ξ, together with the respective error ranges. For the system under study LC-pAc, the situation is favorable. Approaching T_c leads to small changes of tan Ψ but a large shift in φ_B ($\approx 0.2°$). This is indicative of the formation of a boundary layer with a large thickness on the order of several hundred angstroms, together with a small (negative) dielectric anisotropy at the surface. Both parameters show up separately. Hence, the result of a data fitting procedure under variation of $\Delta\epsilon$ and γ appears reliable.

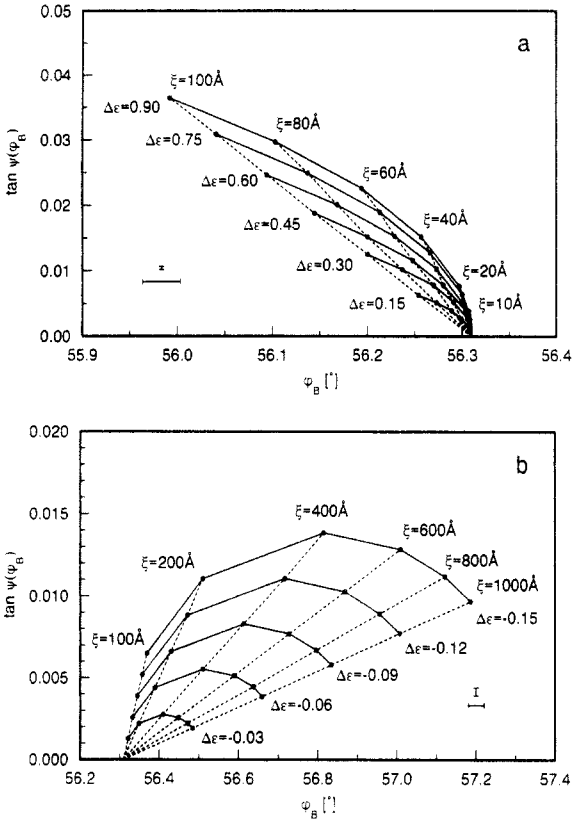

Figure 8. Ellipticity coefficient tan $\Psi(\varphi_B)$ vs Brewster angle φ_B as calculated for the profile given by eq 7 ($\epsilon_b = 2.25$) for positive (a) and negative (b) values of $\Delta\epsilon$. Error bars of experimental values are indicated.

5. Data Evaluation

We have performed a fitting of the curves tan $\Psi(\varphi)$ and $\Delta(\varphi)$ measured at eight different temperatures. In order to account for both the surface roughness and the nematic boundary layer, we assumed as profile function a superposition (by multiplication) of the two profiles in eq 6 and eqs 7 and 8

$$\epsilon_z(z) = \frac{1}{2}\left(1 + \tanh\frac{z}{\gamma}\right)\epsilon_z^{n}(z) \tag{10}$$

$$\epsilon_x(z) = \frac{1}{2}\left(1 + \tanh\frac{z}{\gamma}\right)\epsilon_x^{n}(z) \tag{11}$$

with

$$\epsilon_z^{n}(z>0) = \epsilon_b + (2/3)\Delta\epsilon_0 \exp(-z/\xi)$$

$$\epsilon_z^{n}(z\leq 0) = \epsilon_b + (2/3)\Delta\epsilon_0$$

$$\epsilon_x^{n}(z>0) = \epsilon_b - (1/3)\Delta\epsilon \exp(-z/\xi)$$

$$\epsilon_x^{n}(z\leq 0) = \epsilon_b - (1/3)\Delta\epsilon_0$$

The roughness parameter γ was assumed as independent of temperature. The bulk dielectric constant ϵ_b changes with temperature due to thermal expansion. The change can be derived from the temperature dependence of tan Ψ at angles away from the Brewster angle range. We found a value

$$d\epsilon_b/dT = -9 \times 10^{-4}\ K^{-1}$$

For the highest three temperatures of the series (116.8, 177.0, and 117.5 °C) the curves tan $\Psi(\varphi)$ and $\Delta(\varphi)$ remain unchanged. It appears that the effect of the nematic boundary layer here is negligible. We therefore used these curves for a determination of the constant parameters γ and ϵ_b (T = 117.5 °C). Application of a standard nonlinear fit procedure yielded the values

$$\gamma = 15.2 \pm 0.6\ \text{Å}$$

$$\epsilon_b = 2.5287 \pm 0.0002$$

The temperature-dependent parameters $\Delta\epsilon(T)$ and $\xi(T)$ were then derived from the measurements at T = 116.0–116.4 °C by a curve fitting. The results are given in Figures 9 and 10. One observes low negative values for the anisotropy at the surface, $\Delta\epsilon_0$, and quite large values for the decay length ξ. Figure 11 gives the resulting profiles in terms of the anisotropy $\Delta\epsilon(z) = \epsilon_z(z) - \epsilon_x(z)$. Figure 12 demonstrates that the model provides a good representation of the measured curves.

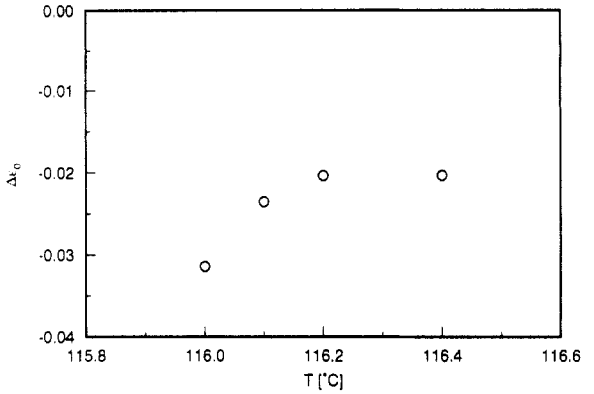

Figure 9. LC-pAc isotropic phase. Temperature dependence of the anisotropy $\Delta\epsilon_0$ at the surface.

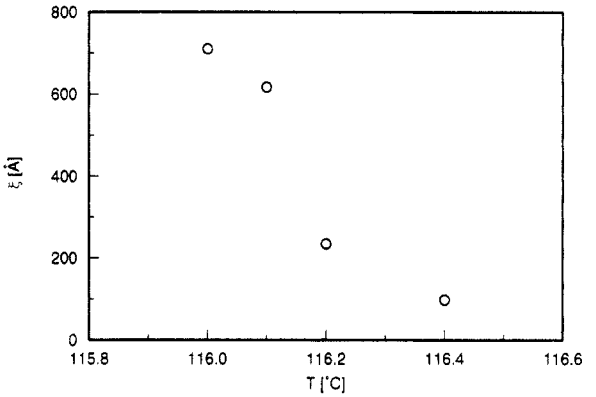

Figure 10. LC-pAc isotropic phase. Temperature dependence of the thickness ξ of the nematic boundary layer.

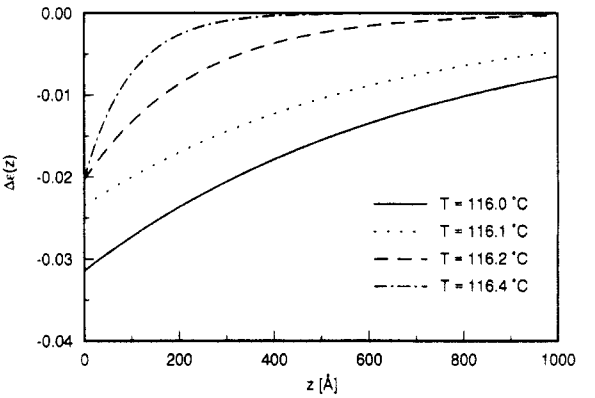

Figure 11. Profiles of the nematic boundary layer corresponding to the parameters given in Figures 9 and 10.

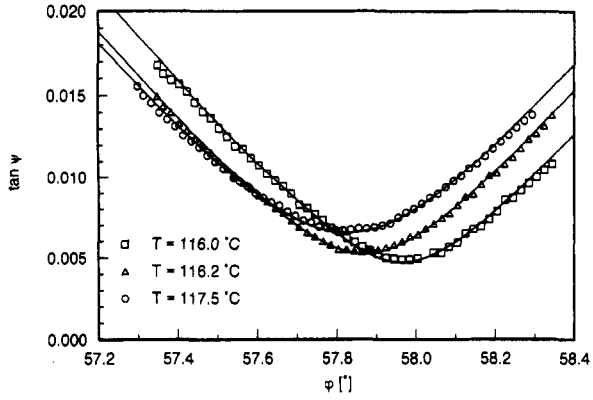

Figure 12. LC-pAc. Representation of measured curves tan $\Psi(\varphi)$ by the model calculation.

6. Discussion

The data evaluation, together with the model considerations presented in section 4, provides evidence for the formation of a nematic boundary layer in the vicinity of T_c. The layer possesses a planar orientation; i.e., the LC side groups are preferentially oriented along the surface. The degree of orientation is only small; the thickness of the boundary layer, however, is quite large, with values on the order of several hundred angstroms.

There is a pronounced increase of the surface excess order on approaching T_c. For the LC polymer under study, which shows a broader transition range than low molecular weight nematogens, it appears difficult to discriminate between a complete wetting, which would be indicated by a divergence of the boundary layer thickness, and critical absorption, associated with a finite thickness at T_c. A distinction on the basis of the different profiles expected for the two different surface ordering mechanisms is also unfeasible. It was possible to determine separately the anisotropy at the interface and the boundary layer thickness, but more detailed information on the profile can hardly be obtained.

The question of the state of order at a free surface and, in particular, of the preferred molecular orientation, homeotropic or planar, has been recently discussed by Tjipto-Margo et al.[14] The molecular alignment in the boundary layer is related to the spatial orientation dependence of the intermolecular potential. In the framework of the Maier–Saupe theory, the (attractive) interaction energy depends only on the angle enclosed by the long axes of the two molecules (for a constant distance) and is isotropic with regard to the relative positions of the centers. No preferred surface orientation is expected in this case. The situation changes if the interaction is spatially anisotropic, i.e., if the interaction depends also on the direction of the intermolecular vectors (relative to the long axes). Theory predicts a planar orientation if the potential energy between two equally oriented molecules is at its minimum for a collinear setting (one molecule above the other). A homeotropic orientation in the boundary layer is expected if the minimum occurs for the side by side position. Differences in the interaction energy may well exist between low molecular weight and polymeric nematogens and result in the observed different boundary layer orientations.

There are two possible forms of a nematic boundary layer with planar orientation.[14] In the first case the nematic director is oriented along the surface normal; there is a total disordering of the molecular orientations with respect to directions parallel to the surface. The second case is given if the nematic director is aligned parallel to the interface. In this case the uniaxial symmetry with the surface normal as the symmetry axis is broken. There were no indications in the experiment speaking for a breakdown of the uniaxial symmetry. Hence, we either deal with the first case or the second case with variable director orientations within the surface region probed by the laser beam (1 mm^2). A distinction appears difficult. The data evaluation was based on the simpler system, given by the first case.

A last remark refers to the large value found for the boundary layer thickness ξ. Principally, not only the LC side groups but also the polyacrylate main chain will show a preferred orientation, either within or normal to the surface. The large values for ξ can be understood as an indication for a preferential orientation of the main chain normal to the surface.

Acknowledgment. We have greatly benefited from discussions with S. Dietrich (University Wuppertal, Germany). Support of this research by the Deutsche Forschungsgemeinschaft (Sonderforschungsbereich 60, Freiburg, Germany) is gratefully acknowledged.

References and Notes

(1) Pershan, P. S.; Braslau, A.; Weiss, A. H.; Als-Nielsen, J. *Phys. Rev. A* **1987**, *35*, 4800.
(2) Ocko, B. M.; Braslau, A.; Pershan, P. S.; Als-Nielsen, J.; Deutsch, M. *Phys. Rev. Lett.* **1986**, *57*, 94.
(3) Miyano, K. *Phys. Rev. Lett.* **1979**, *43*, 51.
(4) Chen, W.; Martinez-Miranda, L. J.; Hsiung, H.; Shen, Y. R. *Phys. Rev. Lett.* **1989**, *62*, 1860.
(5) Beaglehole, D. *Mol. Cryst. Liq. Cryst.* **1982**, *89*, 319.
(6) Sheng, P. *Phys. Rev. A* **1982**, *26*, 1610.
(7) Allender, D. W.; Henderson, G. L.; Johnson, D. L. *Phys. Rev. A* **1981**, *24*, 1086.
(8) Mauger, A.; Zribi, G.; Mills, D. L.; Toner, J. *Phys. Rev. Lett.* **1984**, *53*, 2485.
(9) Telo da Gama, M. M. *Mol. Phys.* **1984**, *52*, 585.
(10) Immerschitt, S.; Koch, T.; Stille, W.; Strobl, G. *J. Chem. Phys.* **1992**, *96*, 6249.
(11) Azzam, R. M. A.; Bashara, N. M. *Ellipsometry and Polarized Light*; North-Holland, Amsterdam, The Netherlands, 1977.
(12) Lekner, J. *Theory of Reflection*; Martinus Nijhoff, Dordrecht, The Netherlands, 1987.
(13) Beaglehole, D. *Physica* **1980**, *100B*, 163.
(14) Tjipto-Margo, B.; Sen, A. K.; Mederos, L.; Sullivan, D. E. *Mol. Phys.* **1989**, *67*, 601.

Registry No. (LC-pAc) (homopolymer), 83847-13-6.